Formation of Yogurt Microstructure and Three-Dimensional Visualization as Determined by Confocal Scanning Laser Microscopy

A. N. HASSAN, J. F. FRANK,[1] M. A. FARMER,[2] K. A. SCHMIDT,[3] and S. I. SHALABI[4]
Department of Food Science and Technology
University of Georgia
Athens 30602-2106

ABSTRACT

Confocal scanning laser microscopy was used to observe coagulum formation resulting from milk acidification. Reconstituted nonfat dry milk was steamed for 15 min, inoculated with yogurt culture or mixed with glucono-δ-lactone, and incubated at 40°C on a warm microscope stage. The pH was monitored on the slide simultaneously with observation of gel microstructure development. Coagulum formation was observed as a continuous process; gelation of the milk was initiated at pH 5.35, as determined by casein micelle aggregation and the cessation of bacterial cell movement. As the pH continued to drop, nonreflective, casein-free spaces around encapsulated microorganisms increased, which was attributed to contraction of the casein network. Direct-acidified milk at pH 5.0 had a three-dimensional microstructure with more uniform sizes and distribution of nonreflective spaces than did cultured yogurt. At pH 4.4, the structural differences between the various acidified milk gels were less apparent. The pH gradient within the milk gel was observed using a fluorescent molecular probe that was sensitive to pH. Areas of relatively high pH corresponded to the light-reflecting areas of the gel, confirming their identity as casein.

(**Key words**: yogurt, microstructure, confocal scanning laser microscopy)

Abbreviation key: **CSLM** = confocal scanning laser microscopy, **GDL** = glucono-δ-lactone.

INTRODUCTION

Acid coagulation is an important chemical property of milk casein. The mechanism by which acid coagulation occurs is not completely understood. Various methods have been used to obtain a dynamic measurement of the coagulation process, including measurements of viscosity and light scattering (1). However, direct observation of gel structure would provide more complete information about protein changes during gelation. Scanning electron microscopy is a useful technique to study milk gel microstructure because of its high resolution and its ability to characterize surfaces as well as internal structures (3, 9). However, milk gels, which have high water contents, must be sufficiently dehydrated before they can be analyzed using electron microscopy (4, 10), and dehydration may change the initial microstructure (12). In addition, other sample preparation steps may alter the natural structure and lead to the creation of artifacts.

Confocal scanning laser microscopy (**CSLM**) enables samples to be observed without preparation procedures (7). This new technique forms a bridge between conventional light microscopy, with its ability to image hydrated live specimens but with limited resolution, and electron microscopy, with its greater resolution but need for extensive specimen preparation (2). The possibility to examine fully hydrated samples, to produce optical sections of these samples, and to utilize digital data to produce three-dimensional images makes CSLM a potentially useful technique

Received February 2, 1995.
Accepted August 21, 1995.
[1]Corresponding author.
[2]Center for Advanced Ultrastructural Research.
[3]Department of Animal Science and Industry, Kansas State University.
[4]Food Technology and Dairy Science Department, University of Minia, Egypt.

for observing milk gel microstructure. In addition, the formation of milk gel as a function of pH and temperature can be monitored while obtaining CSLM data.

The objectives of this study were to apply CSLM to observe yogurt microstructure and to monitor structure development of yogurt and direct-acidified gel in real time. In addition, pH gradients in yogurt were observed.

MATERIALS AND METHODS

Monitoring of Yogurt Microstructure

An MRC-600 confocal scanning laser microscope (Bio-Rad Inc., Hertfordshire, England) with a 60 times oil immersion objective (1.4 numerical aperture) and an Ar/Kr laser (Bio-Rad Inc.) operating in the reflectance mode was used to monitor the gel structure development in cultured and direct acidified milk. Reconstituted skim milk (11% wt/vol) was steamed for 15 min and then cooled to 44°C. *Streptococcus thermophilus* 3855S and *Lactobacillus delbreukii* ssp. *bulgaricus* 3855L (encapsulated strains obtained from Rhône-Poulenc Dairy Ingredients, Madison, WI) at 2.5% (vol/vol) of each, *Streptococcus thermophilus* 4 (unencapsulated strain isolated from commercial yogurt) at 5% (vol/vol) or 2% (wt/vol) of glucono-δ-lactone (**GDL**; Sigma Chemical Co., St. Louis, MO) were added. Approximately 7 ml of milk mixture were dispensed into a glass chamber in which a pH microelectrode (3.5 × 183-mm stem; Cole-Parmer Instruments Co., Niles, IL) was inserted. The chamber was prepared and incubated at 40°C on the microscope stage. The pH was monitored as the gel structure developed. Images at various pH conditions were digitally captured as 8-bit 768 × 512 data files.

Three-Dimensional Visualization

Yogurt and direct-acidified milk mixes were dispensed to fill completely a glass cylinder, which was covered with a coverslip and incubated upside down at 440°C. This procedure prevented formation of a whey layer between the yogurt and the coverslip, thus allowing optical sectioning of the gel to a greater depth. The chamber with sample was cooled to 4°C after the pH reached 5.0 or 4.4. Optical sectioning of the yogurt and direct-acidified gel samples was initiated 10 μm beneath the coverslip using the reflectance mode. The focus mechanism was stepped in 1.0-μm increments; 20 optical sections were digitized and stored. For volumetric rendering, a set of 60 optical sections with a spacing of .6 μm (resulting in .6-μm^3 data points or "voxels") was acquired. Volume renderings of the samples were created using Voxel View E Software (Vital Images Inc., Fairfield, IA) on a 4035G IRIS Workstation (Silicon Graphics, Mountain View, CA).

Visualization of the pH Gradient

A fluorescent molecular probe [CL-NERF (7′-chloroderivative rhodol); Molecular Probes, Inc., Eugene, OR] that was sensitive to pH was added to the mixes to a final concentration of 2.0 μ*M*. Chambers were incubated upside down at 40°C until a pH of 4.2 was reached. Confocal scanning laser microscopy in the fluorescent mode with a 488-nm excitation wavelength was used to observe the pH gradient in optical sections of the gel.

RESULTS AND DISCUSSION

The ability of the CSLM to visualize the live encapsulated microorganisms as well as the casein micelles (6) made it possible to follow the coagulation of milk in real time. Unencapsulated microorganisms could not be seen because they were obscured by the casein micelles (data not shown). Simultaneous monitoring of changes in pH and microstructure development was made possible by inserting a microelectrode into a glass chamber that fitted onto the microscope stage. Observation of samples about 10 to 15 μm beneath the cover-slip avoided surface reflection effects and allowed the acquisition of sharp images. The focal plane was held constant during acidification. Examples of optical sections taken during acidification are presented in Figure 1.

At pH 6.4, encapsulated microorganisms were surrounded by nonreflecting zones (6) within the reflective casein micelles. An increase in the number of microorganisms per field was associated with a drop in pH from 6.4 to 5.5. At this pH range, the casein micelles appeared to be uniform in size and distribution (Figure 1, a and b). At pH 5.5, movement of microorganisms decreased, and the casein became coarser, indicating the initiation of aggregation.

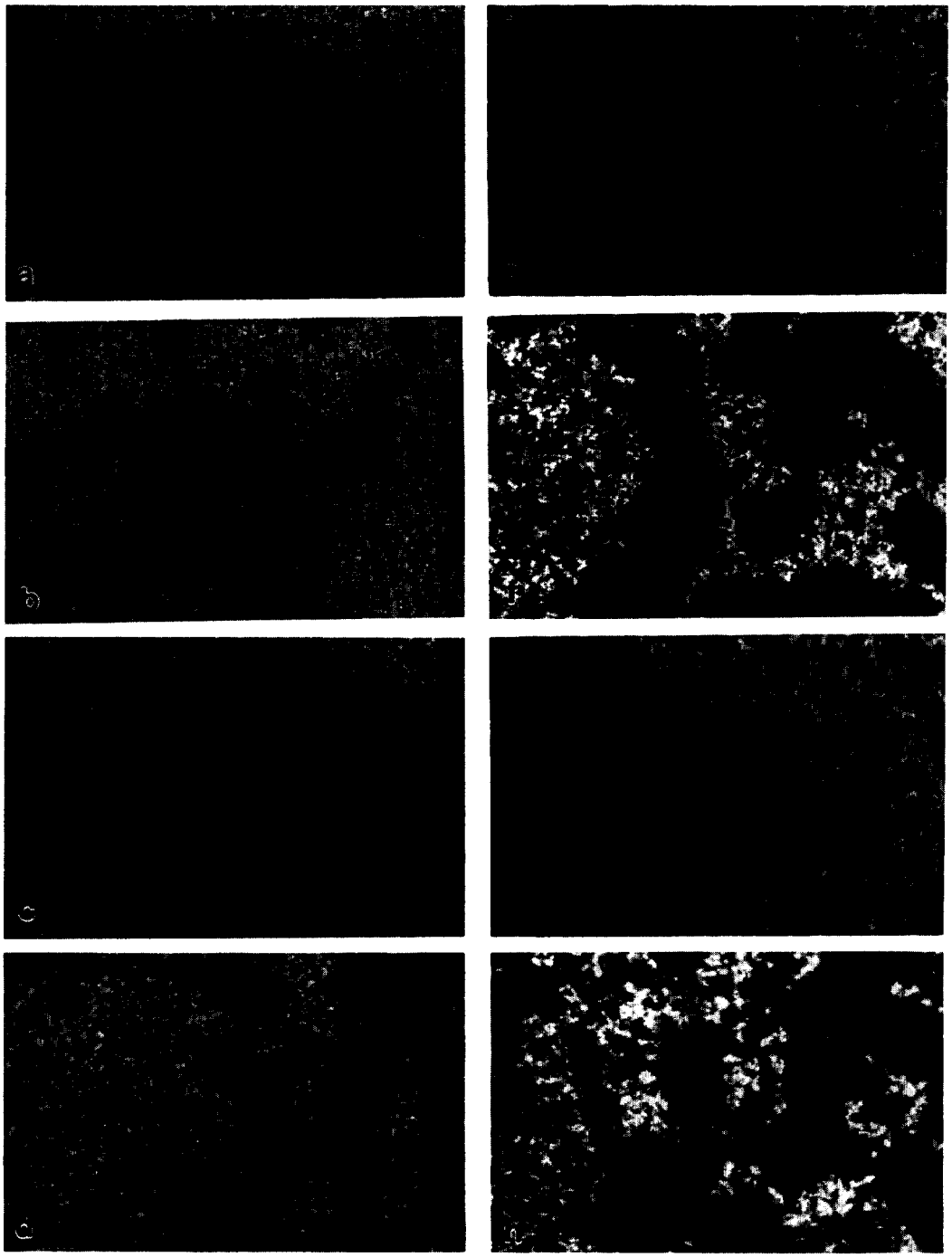

Figure 1. Photomicrographs of microstructure development in direct-acidified milk (a, c, e, and g) and yogurt made using encapsulated starter (b, d, f, and h), obtained by using confocal scanning laser microscopy in reflectance mode. a and b, pH 5.56; c and d, pH 5.35; e and f, pH 5.12; and g and h, pH 5.0. Bar = 10 μm.

When the pH reached 5.35, the milk was viscous enough to stop microbial movement completely, and the casein appeared as large micelle aggregates separated by nonreflective (black) spaces (Figure 1, c and d). At this point, a contraction was initiated, resulting in smaller masses of casein aggregates with a more porous structure and larger nonreflecting zones around the encapsulated microorganisms (see arrows; Figure 1, d and f). At pH 5.35, the casein aggregates initiated formation of a three-dimensional network composed of clusters and chains.

At pH 5.0, milk coagulation caused a thin layer of the whey to form between the coverslip and the gel, making image collection no longer possible. Structural differences in the yogurt resulted from the presence of encapsulated microorganisms producing a product that was structurally different from the direct-acidified product (compare Figure 1, g and h). The microstructure of milk gel produced using unencapsulated *S. thermophilus* was similar to that produced by direct acidification (data not shown). The casein micelles aggregated around the encapsulated microorganisms, leaving large zones of nonreflecting spaces surrounded by masses of porous casein aggregates. In the direct-acidified gel, aggregation produced a more continuous structure with uniform size and distribution of the pores.

The constant size of the nonreflective zones around the encapsulated microorganisms from pH 6.4 until casein contraction, followed by an increase in the size of these zones, explains the origin of the void spaces associated with culture microorganisms that have previously been observed in yogurt by scanning electron microscopy (10). These zones originated with bacterial capsules and then increased in size as a result of aggregation and contraction of the casein away from the microorganisms and their capsules. Therefore, the nonreflecting zones contained both the bacterial capsule and

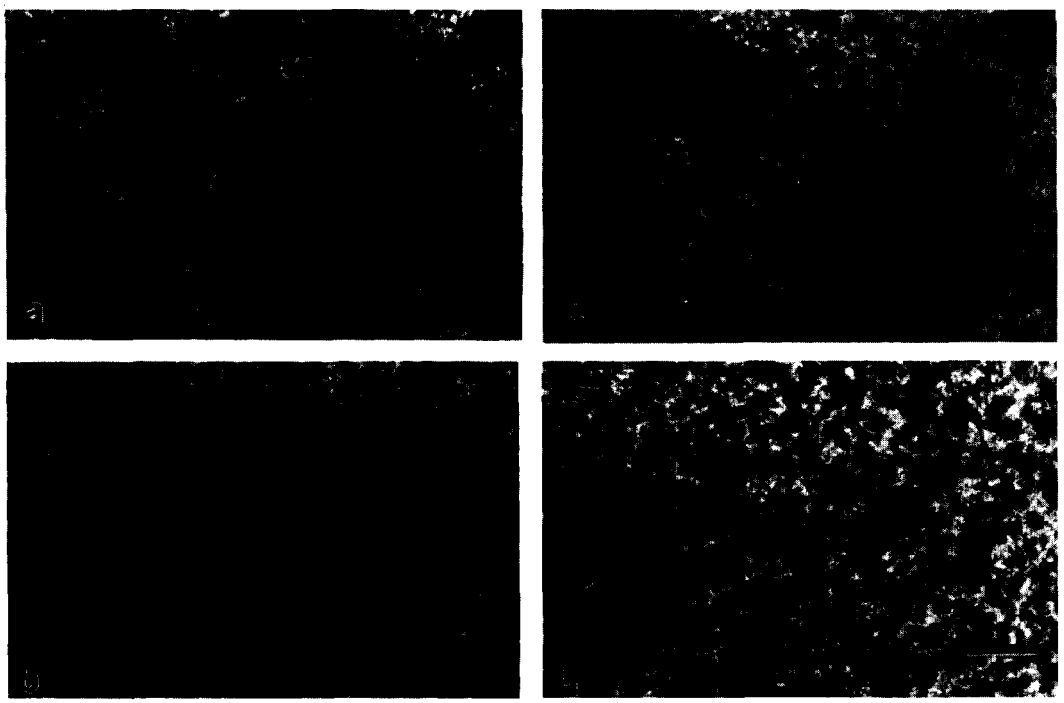

Figure 2. Optical sections of yogurt made using encapsulated culture (a and c) and direct-acidified gel (b and d) at pH 5.0. a and b, 25-μm depth; and c and d, 35-μm depth. Sections were obtained by using confocal scanning laser microscopy in reflectance mode. Bar = 10 μm.

milk serum. We have no evidence that the bacterial capsule increased in size during the yogurt fermentation. In addition, the distribution of the microorganisms in the final gel structure was similar to distribution just prior to the contraction stage.

Confocal images could only be cautiously compared with those obtained by scanning electron microscopy because confocal microscopy shows the overall gel structure but not the details of the casein micelle structure. Heertje et al. (8) used the freeze-fracture technique and reported steps in acid coagulation that were similar to those observed by us in our study. Scanning electron microscopy produced additional details, such as a stage prior to micelle aggregation in which weakly bound β- and κ-caseins dissociate from the micelles while a size-determining micellar framework of α_s-casein remains intact, resulting in little decrease in particle size but in an increase in micelle voluminosity. This dissociation step was not observed in the confocal images because of the more limited resolution of this technique. Parnell-Clunies et al. (11) used transmission electron microscopy to study the gelation profiles of yogurt and confirmed the findings of Heertje et al. (8), who followed the structure formation in direct-acidified milk gel. Those researchers did not report differences in the microstructure development of cultured yogurt compared with direct-acidified gel. Although transmission and scanning electron microscopic images show greater details, such as individual casein micelle sizes, disintegration of micelles into submicelles, and the development in the aggregate sizes, CSLM methodology can determine the precise pH at which coagulation steps occur. Observation of the same microscopic field throughout coagulation showed the movement of casein aggregates and microorganisms from aggregation to coagulation.

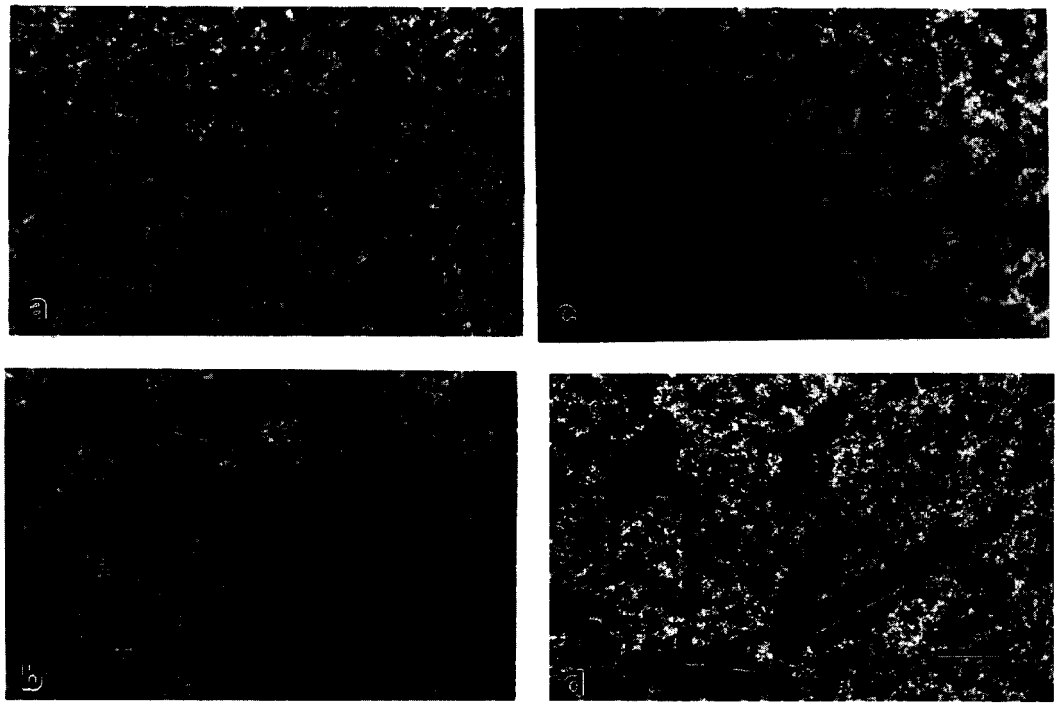

Figure 3. Optical sections of yogurt made using encapsulated culture (b and d) and direct-acidified gel (a and c) at different pH conditions: a and b, pH 5.0; c, pH 4.33; and d, pH 4.4 Sections were obtained by using confocal scanning laser microscopy in reflectance mode. Bar = 10 μm.

Final Structure of Acid Milk Gel

Optical sections showing the internal structure of undisturbed acid gels are presented in Figure 2. The structure of yogurt made with encapsulated strains was dependent on the distribution of microorganisms within the protein matrix. Microorganisms could be observed within pores. Figure 3 shows the microstructure of milk gels at different pH conditions. As the pH dropped from 5 to 4.4, the microstructure of the cultured yogurt became finer and more porous, exhibiting a more well-defined continuous casein network composed of smaller particles linked into a three-dimensional network via particle chains (Figure 3d). At pH 4.4, aggregates had more pores and smaller nonreflective zones around the microorganisms than did the gel at pH 5.0. These smaller nonreflective zones might be a result of additional contraction of the casein network, leading to rearrangement of the casein around the bacterial cells. Harwalker and Kalab (5) proposed that the increased positive charge of the casein micelle at low pH reduced intermicellar interactions, resulting in the formation of a more porous structure. As the nonreflective spaces decreased in size, direct contact between the aggregates and the microorganisms was minimal, possibly because of the presence of the cell capsule. As the pH dropped from 5 to 4.33 in the direct-acidified gel (Figure 3c), the structure became more porous, and fusion of casein particles into chains became greater. The direct-

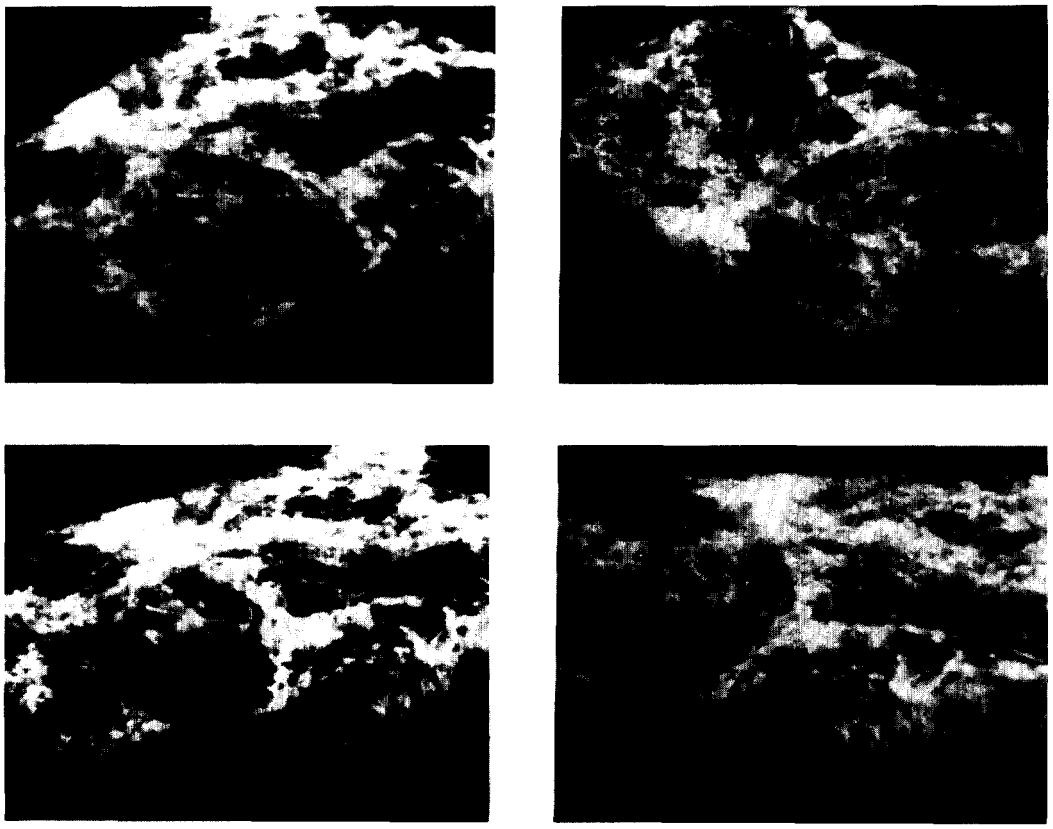

Figure 4. Volume rendering of yogurt made using encapsulated culture rotated to give different views compiled from 60 optical sections obtained by using confocal scanning laser microscopy in reflectance mode. The rendered section is approximately 36-μm thick.

acidified structure exhibited uniform distribution of the pores and the casein aggregates. At low pH, the effects of using an encapsulated culture were less apparent than at higher pH.

Figure 4 presents various rotations of a cubic rendering of yogurt made with encapsulated culture. With cubic rendering, each data point represents a cubic volume in the sample (i.e., the rendering carries information about x, y, and z dimensions). As a result, the images appeared without spaces between optical sections. The volumetric images showed a sponge-like texture with a nonuniform structure and large nonreflecting zones surrounding the microorganisms. The side view showed the distribution and depth of these zones.

The pH gradient within milk gels was observed using the fluorescent molecular probe, CL-NERF, which is sensitive to pH. The CL-NERF molecule is soluble in water, does not penetrate bacterial membranes, and is nontoxic to the culture. The false color images in Figure 5 show variations in fluorescence intensity resulting from the presence of the probe. These images are thin optical sections of yogurt (made using encapsulated culture) and direct-acidified gels at about 20-μm depth. Blue areas indicated a relative lack of fluorescence from inhibition of probe fluorescence by low pH. Red and orange areas indicated buffering zones where fluorescence was not suppressed as much. The buffered areas corresponded to the

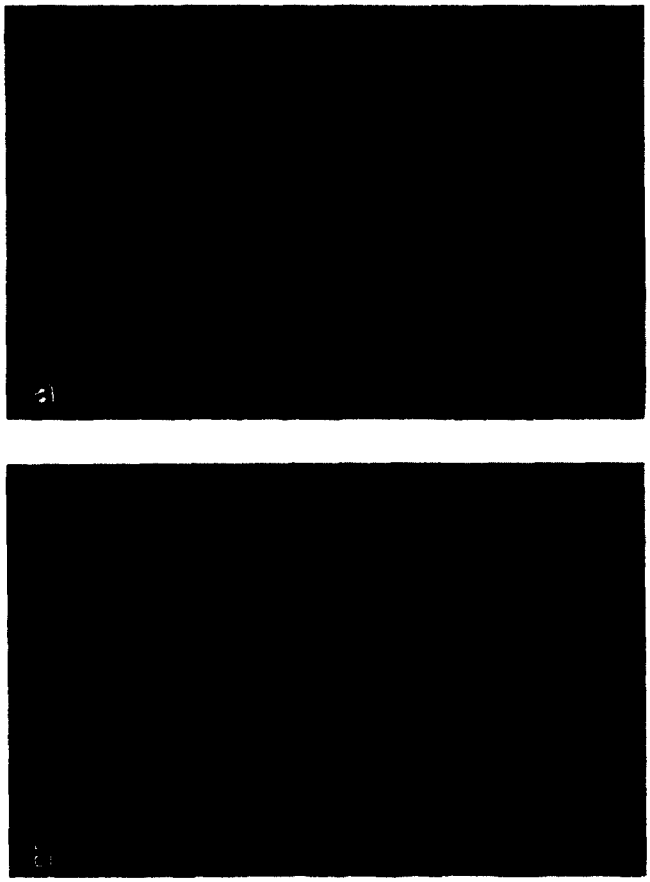

Figure 5. False color visualization of pH gradients in optodigital thin sections of direct-acidified gel (a) and yogurt with encapsulated culture (b), obtained using a CL-NERF molecular probe (Molecular Probes, Inc., Eugene, OR) and confocal scanning laser microscopy in fluorescent mode. Red-orange indicates relatively high pH, and blue-black indicates relatively low pH (see color scale bar). Bar = 10 μm.

light-reflecting areas of the gel that were observed with CSLM in reflectance mode, therefore confirming the accuracy of the reflectance results. Because CL-NERF did not penetrate bacterial cells, their visibility in Figure 5b indicated that cell surfaces were at a higher pH than the surrounding whey. The pH gradient associated with bacterial capsules that was observed by Hassan et al. (6) in fermenting milk at pH 5.5 was not apparent in the finished product at pH 4.2. The lactobacilli used to make the yogurt shown in Figure 5b produced a capsule of only 1.5 μm in diameter, which would not be visible in this photomicrograph. The streptococci used to make this yogurt produced 4- to 5-μm diameter capsules, but those organisms were not definitively identified in the photomicrographs. In finished yogurt, unlike in the initial fermentation (6), the pH differential between the capsule and the whey was possibly too small to allow capsule visualization by this methodology.

CONCLUSIONS

Confocal scanning laser microscopy was a useful technique to visualize the formation and three-dimensional microstructure of yogurt gels in their natural, fully hydrated state. The CSLM allowed observation of milk coagulation in real time. While milk coagulation was monitored, three stages were observed: lag phase, aggregation, and contraction with rearrangement. Encapsulated microorganisms acted as nuclei for the formation of the nonreflective zones within the gel. Direct-acidified gel and gels made using unencapsulated culture exhibited a more uniform structure with a more even distribution of pores than did yogurt made with encapsulated cultures, the porosity of which was dependent on the distribution of the microorganisms. Structural differences between the milk gels were fewer as the pH dropped from 5 to 4.4. Confocal images can provide information for understanding the physical properties of milk gels. In addition, the ability to observe structural changes in real time as a function of pH makes CSLM a useful tool for understanding factors affecting both microstructure and physical stability of cultured milk products.

ACKNOWLEDGMENTS

This research was supported by the Egyptian government through a Channel Grant program between Minia University and The University of Georgia. Additional support was provided by state and Hatch funds allocated to the Georgia Agricultural Experiment Stations.

REFERENCES

1 Banon, S., and J. Hardy. 1992. A colloidal approach of milk acidification by glucono-δ-lactone. J. Dairy Sci. 75:935.
2 Brankenhoff, G., H. Van der Voort, E. Van Sponsen, and N. Nanninga. 1988. 3-Dimensional imaging of biological structures by high resolution confocal scanning laser microscopy. Scanning Microsc. 2:33.
3 Brooker, B. E., and K. Wells. 1984. Preparation of dairy products for scanning electron microscopy: etching of epoxy resin-embedded material. J. Dairy Res. 51:605.
4 Buccheim, W. 1982. Aspects of sample preparation for freeze-fracture and freeze-etch studies of proteins and lipids in food systems. A review. Food Microstruct. 1:189.
5 Harwalkar, V. R., and M. Kalab. 1986. Relationship between microstructure and susceptibility to syneresis in yogurt made from reconstituted nonfat dry milk. Food Microstruct. 5:287.
6 Hassan, A. N., J. F. Frank, M. A. Farmer, K. A. Schmidt, and S. I. Shalabi. 1995. Observation of encapsulated lactic acid bacteria using confocal scanning laser microscopy. J. Dairy Sci. 78:2624.
7 Heertje, I., P. Van der Vlist, J.C.G. Blonk, H.A.C.M. Hendricks, and G. J. Brakenhoff. 1987. Confocal scanning laser microscopy in food research: some observations. Food Microstruct. 6:115.
8 Heertje, I., J. Visser, and P. Smits. 1985. Structure formation in acid milk gels. Food Microstruct. 4:267.
9 Kalab, M. 1981. Electron microscopy of milk products: a review of techniques. Scanning Electron Microsc. 3:453.
10 Kalab, M., P. Allan-Wojtas, and B. Phipps-Todd. 1983. Development of microstructure in set-style nonfat yogurt. A review. Food Microstruct. 2:51.
11 Parnell-Clunies, E., Y. Kakuda, J. M. DeMan, and F. Cazzola. 1988. Gelation profiles of yogurt as affected by heat treatment of milk. J. Dairy Sci. 71:582.
12 Schmidt, D. 1982. Electron microscopy of milk and milk products: problems and possibilities. Food Microstruct. 1:151.